A rheological model for spheroids including extra-cellular matrix

Claude Verdier, Liviu Iulian Palade

Cite this: DOI: 00.0000/xxxxxxxxxx

A rheological model for spheroids including extra-cellular matrix†

Claude Verdier,*[a] and Liviu Iulian Palade[b]

Received Date
Accepted Date

DOI: 00.0000/xxxxxxxxxx

The rheology of spheroids has been studied intensively recently and it was shown that the presence of the extra-cellular matrix (ECM) can have significant effects on the overall behaviour of these biological systems. Collagen-I can indeed be a proxy between cells and bring new intriguing effects, as its content increases. To investigate these effects further, a two-phase emulsion model is proposed including interactions between cells and the ECM. Starting with the single cell and collagen individual viscoelastic properties, such a model can be tested against previously obtained data for spheroids. The model has interesting features and capabilities for it covers a variety of behaviours and uses fitting parameters such as cell concentration and interfacial tension. It is shown that the final intercellular collagen content can be large as compared to the initial one, and that an increase in collagen content induces a larger packing of cells.

1 Introduction

Spheroids are very interesting 3D biological systems, and good candidates to describe tumours[1]. Although there has been a growing interest recently[2–6], their mechanical properties are not yet satisfactorily understood. Indeed, cells packed together correspond to a concentrated suspension[7], but the extra-cellular matrix embedded into the system, or secreted by cells makes the picture harder to describe. In addition cells are viscoelastic, and especially cancer cells are known to exhibit different mechanical signatures[8–13], in particular when in contact with various substrates[6,14] or micro–environments[15]. A few studies have focused on the effect of extra-cellular matrix (ECM) and its potential role to change the rheology of the spheroids. In particular, ECM can be considered as a proxy[16] acting as a porous material drained by water or the culture medium present in the spheroid[17]. But the influence of a larger collagen content may allow the building up of a new microstructure also responsible for the larger mechanical moduli observed[18]. It is definitely accepted that the whole spheroid is viscoelastic, due to the presence of cells embedded within the ECM – a gel-like system – with liquid medium. Probably the best way to model the behaviour of such spheroids is to consider the ECM–water surrounding medium as a gel with viscous and elastic properties. Such ECM properties have been studied extensively in the literature in the linear and nonlinear regimes[19–23]. In addition the gel biopolymers enable cells to bind or adhere within connective tissues or other situations to allow stress transfer[24].

In this work we propose to study spheroids consisting of two phases, i.e. the ensemble of cells and the collagen matrix. We use the matrix mechanical properties as well as individual cell properties in contact with a similar environment, that is to say when they are surrounded by other cells. Then we study the predictions of a viscoelastic emulsion model, valid for large concentrations in order to obtain the whole spheroid rheology. This is carried out in details by varying parameters. Finally we optimize these parameters to predict previous results[18] obtained for spheroids containing an excess of collagen.

2 Materials and methods

Collagen was prepared according to the manufacturer protocol (Corning). Rat tail collagen I was mixed with PBS (1X) and NaOH (1M) was added at 4°C until the correct pH was obtained (7.4). Then it was let to polymerise at 37°C for 30 minutes. These collagen properties were measured as described in previous work[25]. Briefly, classical rheometry tests at 37°C using parallel plate geometry (20mm-diameter) were carried out in oscillatory shear mode in the [0.03Hz-10Hz] range. Then experiments using AFM in force modulation mode were carried out following a previous method[26,27] using indentation of a flat collagen surface (in PBS) with a pyramid AFM tip (half angle $\theta \sim 20°$). An initial indentation δ_0 was applied, followed by small oscillations ($\delta << 1$) in the linear regime, thus allowing to measure the complex shear moduli $G^*(\omega) = \frac{1-\nu}{3\delta_0 tan\theta}\left\{\frac{F^*}{\delta^*} - i\,\omega\, b(0)\right\}$, where G*=G'+iG", G' and G" were respectively the elastic and loss shear moduli, ν was the Poisson ratio ($\nu \sim 0.5$), F^* and δ^* were the complex force and indentation, and the last term was the drag on the surrounding liquid, with b(0) being a coefficient containing the geometry of the system as well as the fluid viscosity[26]. Using these complementary experiments, the range [0.03Hz-1kHz] was covered.

T24 cells (epithelial bladder cancer line) were cultured in RPMI medium with 10% FBS and 1% penicillin-streptomycin. They were seeded on different Polyacrylamide substrates (5, 8, 28 kPa) as well as a biological one, consisting of Human Vascular endothelial Cells (HUVECs), as discussed previously[28]. AFM measurements were carried out with a pyramidal tip (half angle $\theta \sim 20°$) for their viscoelastic shear moduli G' and G" at 37°C (same method as above). The influence of the substrate was taken

[a] Address, Université Grenoble-Alpes, CNRS, LIPhy, 38000 Grenoble, France. Tel: 33 4 76 63 59 80; E-mail: claude.verdier@univ-grenoble-alpes.fr
[b] Address, CNRS, Institut "Camille Jordan", UMR 5208 & Pôle de Mathématiques, INSA-Lyon, Université de Lyon, 69621 Villeurbanne, France. E-mail: liviu-iulian.palade@insa-lyon.fr

into account in order to correct for substrate effects. As it was important to find a relevant micro-environment for these cells, like in a real spheroid, it was preferred to use their properties when they were in contact with the biological substrate, in this case the endothelial cells.

Spheroids were prepared in 15μL hanging droplets containing 5,000 T24 cells in culture medium and collagen (0 or 0.01 mg/mL or 0.03 mg/mL) as described previously[18]. A spheroid was formed after three days. Spheroids were transferred into a Petri dish for AFM measurements at 37°C. A large tipless cantilever (Nanosensors, TL-NCL model, length 225 μm, width 38 μm[6]) was chosen for these measurements in force modulation mode, in order to make a plane-spherical contact. Viscoelastic data was obtained in the range [1Hz-1kHz]. The other spheroids were kept for confocal microscopy imaging.

3 Properties of the collagen matrices

After collecting data from classical rheology and AFM, results were plotted on the same graph, as a function of frequency. Matching of the two tests was found to work nicely as previously shown for PolyAcrylamide samples[27]. Such results are shown in Fig. 1. A typical power-law behaviour[29] was found for both G' and G" at different collagen concentrations (c=1, 2, 4 mg/mL) usually in the range [0.05Hz-10 Hz] and both G' and G" increased faster in the high frequency range. Note that the measured values of the moduli were usually smaller as compared to cell's values[6]. Finally fitting of the data was achieved using simple power-laws as described below.

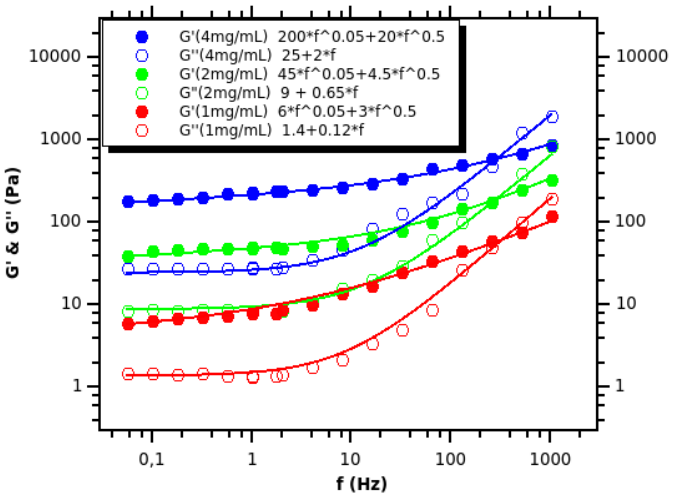

Fig. 1 Rheological properties of the collagen matrix for three concentrations: 1mg/mL, 2 mg/mL and 4mg/mL. Data are collected from classical rheology (0.01 Hz-10 Hz) and AFM rheology (1 Hz-1 kHz).

4 Cell properties

To investigate cell rheology, it was necessary to consider cells in the proper environment as it is known that the micro–environment plays a role on their cytoskeleton organization, therefore changes cellular mechanical properties[6,14]. Cells within a spheroid are surrounded by other cells therefore it is convenient to use such a micro–environment[12]. Unfortunately, using AFM, it is hard to have access to the cell mechanical properties within the tissue, expect if one uses other techniques such as bead tracking microrheology[30]. Here we preferred to use those cells properties (T24 epithelial bladder cancer cells) obtained when in contact with other cells of similar stiffness[6]. Indeed, after studying T24 cells plated on substrates of different stiffness and on endothelial cells, it was found that endothelial cells are the best substrate because they could mimic the environment (see Fig. 1F in previous work[28]). This choice was motivated by our undertaking to represent the dynamic shear properties of the T24 cells used in our spheroids. Fig. 2 below represents the G' and G" moduli obtained as cells are in contact with an endothelium monolayer, with stiffness $\sim$ 8 kPa, corresponding precisely to T24 cell rigidities, E $\sim$ 3 G'(1.4Hz) $\sim$ 8 kPa[28]. This represents closely the micro–environment felt by the cells in the spheroid[12]. The frequency range was chosen from 1 Hz to 1 kHz as was the case in the aforementioned work.

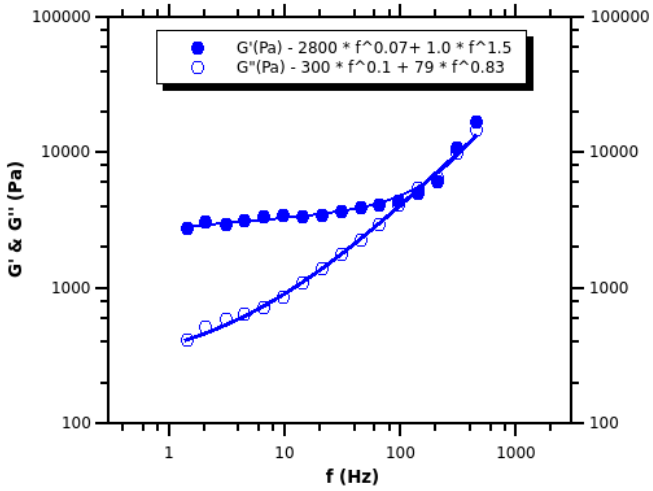

Fig. 2 Rheological data of T24 cells, in contact with an endothelium monolayer, as a close representation of the cell's environment found in a spheroid.

5 Two-phase model with interfacial tension

5.1 Emulsion model

We started with the original work on emulsions carried out by Palierne in the 90s[31,32]. The two–phase model described for polymeric or viscoelastic systems requires the knowledge of complex shear moduli obtained for small deformations, i.e. in the linear regime. The model has been used mainly for two–phase polymeric systems (see for example the work on polymer blends[33]). Nevertheless it may be used for materials such as gels or cellular media exhibiting known viscoelastic properties. Here the medium had a characteristic complex modulus $G^*_m(\omega)$ whereas the inclusions have modulus $G^*_i(\omega)$. The volume fraction of the inclusions is ϕ but different inclusions may be considered with different sizes and concentrations (in case of heterogeneous sizes). Here we assumed that only cells with a typical radius R coexist, which is

usually the case since cell size is roughly constant. In this case, $G^*(\omega)$, the average modulus of the spheroid, i.e. cells embedded in the collagen matrix, is written as, in the case of non-diluted emulsions[31]:

$$G^*(\omega) = G^*_m(\omega)\frac{1+3\phi H^*(\omega)}{1-2\phi H^*(\omega)} \quad (1)$$

where the function $H^*(\omega)$ is defined as:

$$H^*(\omega) = \frac{\frac{4\alpha}{R}[2G^*_m(\omega)+5G^*_i(\omega)]+[G^*_i(\omega)-G^*_m(\omega)]D^*(\omega)}{\frac{40\alpha}{R}[G^*_m(\omega)+G^*_i(\omega)]+[2G^*_i(\omega)+3G^*_m(\omega)]D^*(\omega)} \quad (2)$$

after defining $D^*(\omega) = 16G^*_m(\omega)+19G^*_i(\omega)$.

In this formula, α is the interfacial tension and may be considered here as an interaction energy per unit surface between cells and the matrix. It will be significant when cells adhere a lot to the matrix or are able to make a sufficiently large number of bonds. This should be the case possibly at high collagen content. Note that for the case of dilute emulsions, Eq.2 is different and should be replaced by $G^*(\omega) = G^*_m(\omega)(1+\frac{5}{2}\phi H^*(\omega))$. In particular, this allows to recover the usual Einstein's formula[34] for two Newtonian fluids.

To summarize, we could use this model based on the cell properties $G^*_i(\omega)$ determined previously and the gel properties $G^*_m(\omega)$, known for different collagen I concentrations. Note that the collagen concentration is unknown within the spheroid, and similarly ϕ, the cell concentration is to be determined. ϕ should be large since most of the spheroid is made of cells, and one could expect the ECM content to be in the range 1-15%[5], assuming that cells make their own matrix. The other running parameters are α, the adhesion energy per unit area (in N/m), and R the cell radius, but the latter one is known since such T24 cells usually have a radius of 10μm $\pm$ 1μm.

In a first approximation, we noticed that collagen is much less elastic (and viscous) as compared to the cell behaviour. Therefore, we could neglect the viscoelastic part in Eq (1). This implies that $D^*(\omega) \sim 19G^*_i(\omega)$ and $H^*(\omega) \sim \frac{1}{2}$ therefore $G^*(\omega) \sim G^*_m(\omega)\frac{1+1.5\phi}{1-\phi}$. So $G^*(\omega)$ scales with the matrix complex modulus $G^*(\omega)$, with the prefactor $\frac{1+1.5\phi}{1-\phi}$. Note that a small collagen content like 5% gives $\phi = 0.95$ therefore a prefactor of 48.5. Values of the prefactor are shown in the Table 1 below.

Table 1 Values of the prefactor

ϕ	0.05	0.1	0.3	0.5	0.7	0.9	0.95
$\frac{1+1.5\phi}{1-\phi}$	1.13	1.28	2.07	3.5	6.83	23.5	48.5

This shows that even though the collagen modulus $G^*_m(\omega)$ is rather small (Plateau of G' around 200 Pa), as compared to cell's moduli (Plateau of G' at 2,000 Pa), the amplification due to spherical inclusions such as cells can be large and could lead to the high values obtained in spheroids[18].

The formula originates from analysis of the effect of the adhesion energy α. If α/R becomes very small as compared to the other moduli (and collagen moduli are neglected vs. inclusions moduli) then the function $H^*(\omega)$ again becomes independent of α and is close to 1/2. At this stage, if we briefly compare with the results of our previous work[18], we notice that the moduli increase with collagen content (decreasing ϕ). On the order hand, the previous equation predicts decreasing moduli. Therefore it seems important to consider the effect of all parameters: we consequently check the influence of α/R, ϕ, $G^*_i(\omega)$ and $G^*_m(\omega)$ upon the numerical results.

5.2 Application to the rheology of spheroids

We have at our disposal the data from a previous study where collagen was added when making spheroids[18]. Three initial concentrations were used: 0 mg/mL, 0.01 mg/mL and 0.03 mg/mL. This does not mean that the local collagen content is the same when the spheroids are formed. Indeed spheroids were prepared in hanging droplets rich in collagen and cells used it to adhere and exhibit a round shape. The same T24 cells were used for this study. Fig. 3 shows typical confocal microscopy images of such spheroids elaborated using these three initial collagen contents: 0, 0.01 mg/mL and 0.03 mg/mL. As shown in the red channel, the reflectance of collagen is enhanced at higher collagen content, thus allowing to check the presence of collagen inside the spheroid. Cells (green channel) seem to form nice round spheroids except for the first case where no collagen was added.

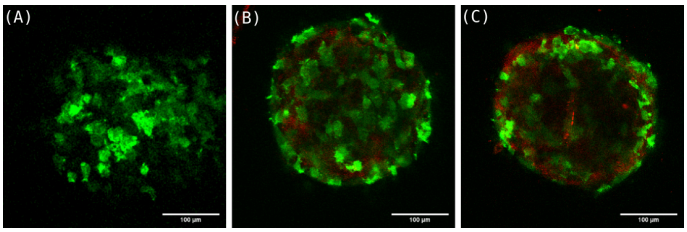

Fig. 3 Confocal microscopy images of spheroids prepared using T24 cells in hanging droplets, containing different initial collagen contents: 0mg/mL, 0.01mg/mL and 0.03mg/mL. Adapted from Tsvirkun *et al.*[18].

We will model the different phases of the spheroid. The first one was collagen. Using the previous data in Fig. 1, it was found that the collagen behaviour varies according to power laws versus frequency f. Fits of our previous data give the respective formulae for the three contents, as also shown in Fig. 1. For 4 mg/mL, we find $G'(f) = 200*f^{0.05}+20*f^{0.5}$ and $G''(f) = 25+2*f$. For 2 mg/mL, $G'(f) = 45*f^{0.05}+4.5*f^{0.5}$ and $G''(f) = 9+0.65*f$, and finally the lowest collagen content, 1mg/mL, gives $G'(f) = 6*f^{0.05}+3*f^{0.5}$ and $G''(f) = 1.4+0.12*f$, where f is in Hz, and G', G'' are in Pascals (Pa). Remarkably, these power law exponents are independent of the concentration, so only the prefactors are different.

Similarly, we predicted the behaviour of the viscoelastic response of T24 cells, as shown in Fig. 2. The moduli behave as $G'(f) = 2800*f^{0.07}+1.0*f^{1.5}$ and $G''(f) = 300*f^{0.1}+79*f^{0.83}$. T24 cells exhibit a plateau at the lowest frequency (1.4Hz) corresponding to an elastic modulus $E \sim 3G' \sim 3(2700) \sim 8100$Pa, similar to the elastic modulus of endothelial cells[28].

Let us now consider the effects of the main parameters. Regarding the effect of modulus G^*_i, cells are assumed to have the behaviour depicted in Fig. 2 so this modulus is fixed. Then the

values of the collagen modulus G_m^* can be changed depending on its content within the gel (see Fig. 1). Finally, the roles of the cell content (ϕ) and the adhesion energy per unit area (α/R) will be studied.

5.2.1 Effect of collagen matrix within the spheroid

Here we consider the case ϕ=0.8 which corresponds to typical cell concentration, as seen for example in Fig. 3. For this case, we used α=10.0 mN/m with $R = 10\mu$m. Plots of G' and G" are shown in Fig. 4.

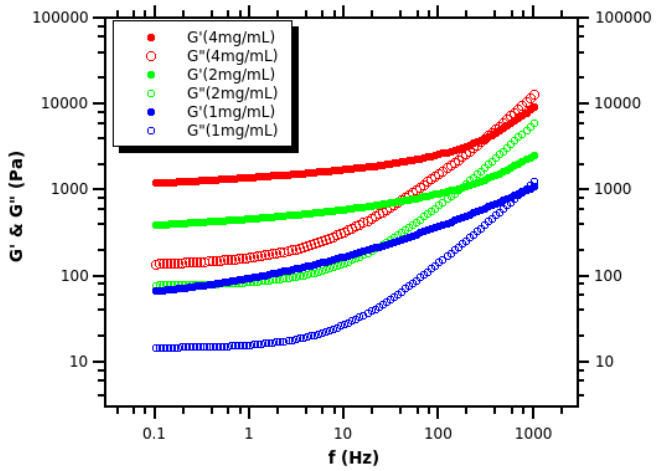

Fig. 4 Predictions of the two–phase emulsion model for 80% cell concentration, α/R=10^3 Pa, at collagen contents 1mg/mL, 2mg/mL and 4mg/mL.

As expected, spheroids moduli increase with collagen content, as could be seen by inspection of formulae (1-2), where the collagen complex viscoelastic modulus $G_m^*(\omega)$ appears as a prefactor. It is found that the resulting properties of the spheroid are in the range of the data previously reported[18], and this will be studied further below.

5.2.2 Role of the cell concentration

Next we studied the role of cell concentration. Usually, in spheroids, cells are closely packed but the presence of collagen, as seen in confocal microscopy (Fig. 3) suggests that the intercellular space can be affected. It has been estimated that the ECM content can sometimes reach $\sim$ 15% in cases where cells make their own ECM[5]. Therefore, we selected typical concentrations between 0% and 20% for the collagen gel, leading to cell concentrations between 80% and 100%. For this case we used the low content of collagen (1mg/mL) and α/R=10^3 Pa. Simulations are shown in Fig.5. It can be concluded that cell concentration has an important effect on the results, especially due the large difference between matrix and cell's moduli.

5.2.3 Effect of adhesion energy between cells and the matrix

Regarding the effect of the adhesion energy, we chose to study realistic values α of 0.3, 3, 30, and 60 mN/m at a cell density of ϕ=0.9, and medium collagen content properties corresponding to 2mg/mL. This is shown in Fig. 6.

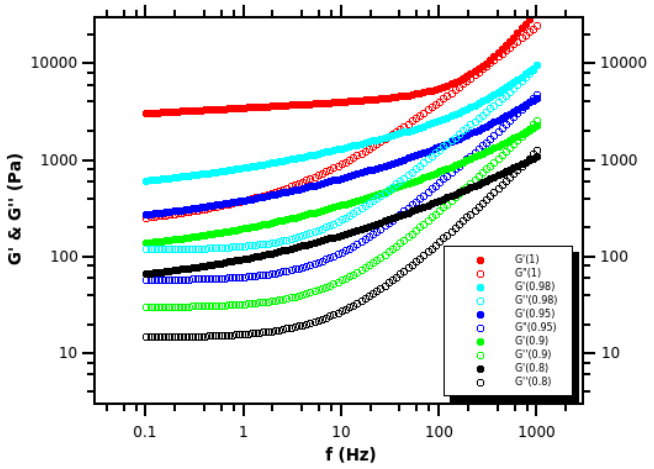

Fig. 5 Predictions of the two–phase emulsion model for various cell concentrations 80%–100%, α/R=10^3 Pa, at 1mg/mL collagen content.

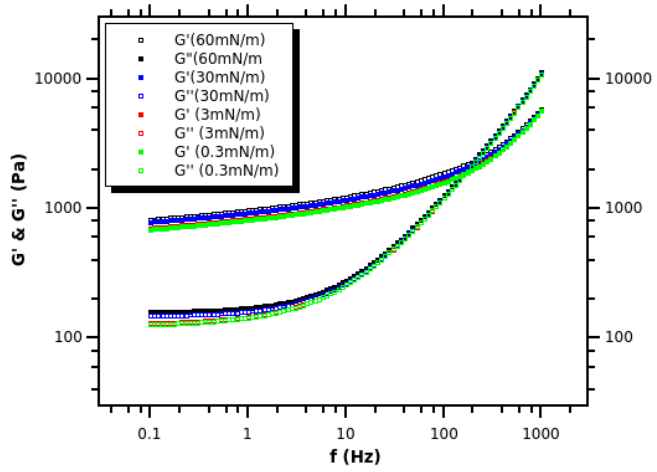

Fig. 6 Predictions of the two–phase emulsion model for various adhesion energies 0.3-3-30-60 mN/m, with R=10 μm, at 2mg/mL collagen content, and ϕ=0.9.

To summarize results from Fig. 6, it appeared that the role of α/R was not so important, with the parameters chosen and the values of the current viscoelastic parameters. Probably this comes from the range of frequencies studied where its effect is not important[33]. Thus α/R was not used extensively to match the final spheroid behaviour, and a mean value of α=30 mN/m was chosen in what follows.

5.2.4 Optimizing emulsion model parameters for real spheroids

Finally, real spheroid properties were considered within the [1Hz-1kHz] range as previously described using AFM microrheology in plane–sphere contact[18]. Measurements were carried out in a manner similar to the one proposed on tissues[35]. Measurements display typical slopes as a function of frequency. To fit the data, parameters were optimized as follows. We adjusted the concentration ϕ (typically between 0.5 and 1) and the collagen

concentration varied from 0 to 4 mg/mL. Results are shown in Fig. 7. Fittings were in very good agreement with experimental data, even though slight discrepancy between data and model predictions are noticed at low frequencies. Here is a summary of the parameters used.

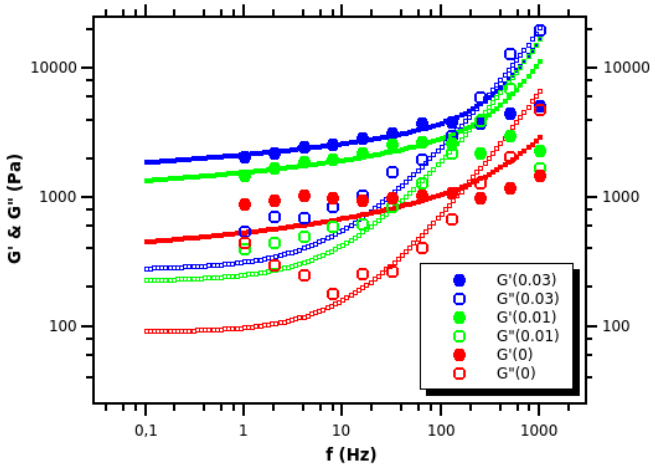

Fig. 7 Spheroid properties for three collagen initial contents 0 mg/mL, 0.01 mg/mL and 0.03 mg/mL (data from previous work[18]). Fits using optimal parameters with the emulsion model: α/R=30mN/m, 2mg/mL collagen content, and respectively ϕ=0.82; ϕ=0.95 and ϕ=0.97.

- **0 mg/mL**. For this case, there is no collagen, but cells secrete their own Extracellular Matrix (ECM) therefore we assumed there was some collagen at a given concentration of 2 mg/mL, which is the optimal concentration for the three cases. We find ϕ=0.82.
- **0.01 mg/mL**. We find that the optimal parameters are ϕ=0.95 and a corresponding concentration of 2 mg/mL.
- **0.03 mg/mL**. We find an optimal ϕ=0.97 for a corresponding collagen concentration of 2 mg/mL.

The table below summarizes these features:

Table 2 Summary of parameters

Initial collagen (mg/mL)	0	0.01	0.03
Optimal ϕ	0.82	0.95	0.97
Intercellullar space	18 %	5 %	3%
Collagen content (mg/mL)	2	2	2
Adhesion energy/unit area (mN/m)	30	30	30

For the 0 mg/mL case, it is probably true that there is a certain amount of ECM as shown in Fig. 3, but cells appear not so much in contact with each others, therefore the 18% volume of intercellular space as predicted by the model seems to be a reasonable value. There is discrepancy in the data as mentioned before[18] because of this lack of adhesion leading to non spherical spheroids.

For the other two cases, an optimal collagen concentration of 2 mg/mL seemed to be a suitable number, in agreement with confocal microscopy (see large amounts of collagen in Fig. 3). Finally cells seemed to be more densily packed in the second case (0.03 mg/mL), meaning that collagen helps cells to bind and plays the role of an interstitial layer enhancing the microstructure as well as the viscoelastic properties.

6 Discussion

The rheological properties of spheroids are of great importance in order to understand how microstructural changes evolve in time, and how such mechanical effects can undergo changes, giving rise to invasion of tumours and/or the formation of metastasis. In addition, their growth is also a topic of major interest[36–39] depending largely on the micro-environment. Interesting studies have shown the effect of collagen on such processes, in particular the micro–environment can be relevant to determine cancer progression and prognosis[40–42]. In this work, we investigated the role of collagen on the viscoelastic properties of spheroids grown during 3 days[18], in culture medium containing an excess collagen I (various concentrations). Using a former model particularly well adapted to viscoelastic behaviour, we studied the possible effects related to ECM (collagen I) density, cell concentration and adhesion effects. This was assessed by modeling frequency–dependent individual cell and collagen properties (Figs 1-2). Based on these properties, we used an emulsion two–phase model[31,32] able to recover the spheroid viscoelastic data.

The effect of collagen (Fig. 4) and cell concentration (Fig.5 were seen to have significant importance whereas the role of adhesion energy (between cells and the matrix) was less significant, due to the frequency range used in the experiments. Indeed a previous work[33] reported this role and found it to be relevant only at lower frequencies, where the terminal relaxation time is a function of surface energy. To improve this feature, other models including poroelastic effects may also be considered[43].

After analyzing the results on three different spheroids[18], prepared with various initial collagen concentrations (0 mg/mL – 0.01 mg/mL – 0.03 mg/mL) we used the emulsion model to optimize the parameters and came up with the best possible fits (Fig. 7). The results of the model were found to be in very good agreement with the experiments. We noted a small discrepancy at the low frequencies for the case of the spheroids prepared without collagen. This was explained by the absence of a dense structure as exhibited on the confocal images (Fig. 3). Still the agreement found was interesting as it motivates further effects in view of the parameters investigated. In particular, the packing of cells within the spheroid seems to be linked with the presence of collagen forming a dense meshwork, enabling cells to connect with each others, in the presence of adhesion molecules (cadherins for instance[44]). As the initial collagen content was increased, it was shown that cells were able to pack more closely – which was rather unexpected – this giving rise to a higher cell content, therefore to higher viscoelastic moduli (see Figs 1-2).

To go beyond this result, we can analyse the ability of the model to predict various slopes, like the ones observed experimentally for cells[26,28,45–48] and spheroids[6,18]. The dependence on frequency at low rates is usually weak for cells or ECM (slopes typically 0.1–0.3), whereas it can become larger at higher frequencies ($\sim$ 1 for G") with a possible exponent of 0.5 for poroelastic

materials[13]. The slopes found here using the model correspond to the complex combination of the viscoelastic properties of both the ECM and the cell's properties. The model leads to a rich variety of spheroid viscoelastic properties, with power–law dependencies[29]. Hence it would be interesting to study spheroids in more in detail in the future, for example when using different cell types or ECM leading to different microstructures[49], or during the growth of tumours[36,38,39]. These microstructures should be minutely analyzed further using confocal microscopy at smaller scales, in order to extract the basic relationships or forces involved in such interactions.

7 Conclusions

The rheology of spheroids has insufficiently been studied so far. Here we used previous viscoelastic data on spheroids measured with an AFM, as well as the individual response of the other components (i.e. cells and collagen). Results were compared with the predictions of an emulsion model including interfacial energy. The results are in very good agreement with the experiments. They show that the final spheroid microstructure contains dense collagen regions within the intercellular spacing. Finally an increase of initial collagen concentration leads to an improved compactness of the spheroids with a smaller intercellular spacing. Thus collagen plays the role of a connecting layer between the cells and improves spheroid stability. With this model, future predictions regarding time–dependent spheroid growth should be possible.

Author Contributions

C.V. carried out data analysis and simulations. Both authors designed research and wrote the manuscript.

Conflicts of interest

There are no conflicts to declare.

Acknowledgements

The authors are thankful to the Nanoscience Foundation (Grenoble) for sponsoring the AFM. C.V. is a member of the LabeX Tec 21, France (Investissements d'Avenir: grant agreement No. ANR-11-LABX-0030). The authors thank D. Tsvirkun and J. Revilloud for interesting discussions.

Notes and references

1 L.-B. Weiswald, D. Bellet and V. Dangles-Marie, *Neoplasia*, 2015, **17**, 1–15.

2 M. Delarue, F. Montel, D. Vignjevic, J. Prost, J.-F. Joanny and G. Cappello, *Biophys. J.*, 2014, **107**, 1821–1828.

3 D. Ambrosi, S. Pezzuto, D. Riccobelli, T. Stylianopoulos and P. Ciarletta, *J. Elasticity*, 2017, **129**, 107–124.

4 L. Guillaume, L. Rigal, J. Fehrenbach, C. Severac, B. Ducommun and V. Lobjois, *Sci. Rep.*, 2019, **9**, 6597.

5 M. Dolega, G. Zurlo, M. L. Goff, M. Greda, C. Verdier, J.-F. Joanny, G. Cappello and P. Recho, *J. Mech. Phys. Solids*, 2021, **147**, 104205.

6 Y. Abidine, A. Giannetti, J. Revilloud, V. M. Laurent and C. Verdier, *Cells*, 2021, **10**, 1704.

7 L. Preziosi, D. Ambrosi and C. Verdier, *J. Theor. Biol.*, 2010, **262**, 35–47.

8 M. Lekka, P. Laidler, D. Gil, J. Lekki, Z. Stachura and A. Z. Hrynkiewicz, *Eur. Biophys. J.*, 1999, **28**, 312–316.

9 S. E. Cross, Y.-S. Jin, J. Rao and J. K. Gimzewski, *Nat. Nanotechnol.*, 2007, **2**, 780–783.

10 M. Plodinec, M. Loparic, C. A. Monnier, E. C. Obermann, R. Zanetti-Dallenbach, P. Oertle, J. T. Hyotyla, U. Aebi, M. Bentires-Alj, R. Y. H. Lim and C.-A. Schoenenberger, *Nat. Nanotechnol.*, 2012, **7**, 757–765.

11 J. Rother, H. Nöding, I. Mey and A. Janshoff, *Open Biology*, 2014, **4**, 140046.

12 K. Gnanachandran, S. Kędracka-Krok, J. Pabijan and M. Lekka, *J. Biomech.*, 2022, **144**, 111346.

13 J.-T. Hang, G.-K. Xu and H. Gao, *Sci. Adv.*, 2022, **8**, eabn6093.

14 J. Solon, I. Levental, K. Sengupta, P. C. Georges and P. A. Janmey, *Biophys. J.*, 2007, **93**, 4453–4461.

15 C. T. Mierke, *Rep. Prog. Phys.*, 2019, **82**, 064602.

16 M. E. Dolega, S. Monnier, B. Brunel, J.-F. Joanny, P. Recho and G. Cappello, *eLife*, 2021, **10**, 1–33.

17 P. A. Netti, S. Roberge, Y. Boucher, L. T. Baxter and R. K. Jain, *Microvasc. Res.*, 1996, **52**, 27–46.

18 D. Tsvirkun, J. Revilloud, A. Giannetti and C. Verdier, *J. Biomech.*, 2022, **141**, 111229.

19 B. R. Dasgupta and D. A. Weitz, *Phys. Rev. E*, 2005, **71**, 021504.

20 P. A. Janmey, M. E. McCormick, S. Rammensee, J. L. Leight, P. C. Georges and F. C. MacKintosh, *Nat. Mater.*, 2007, **6**, 48–51.

21 D. Vader, A. Kabla, D. Weitz and L. Mahadevan, *PLoS One*, 2009, **4**, e5902.

22 C. P. Broedersz, K. E. Kasz, L. M. Jawerth, S. Munster, D. A. Weitz and F. C. MacKintosh, *Soft Matter*, 2010, **6**, 4120–4127.

23 F. Sauer, L. Oswald, A. Ariza de Schellenberger, H. Tzschätzsch, F. Schrank, T. Fischer, J. Braun, C. T. Mierke, R. Valiullin, I. Sack and J. A. Käs, *Soft Matter*, 2019, **15**, 3055–3064.

24 K. L. Goh, J. R. Meakin, R. M. Aspden and D. W. L. Hukins, *J. Theor. Biol.*, 2007, **245**, 305–311.

25 A. Iordan, A. Duperray, A. Gérard, A. Grichine and C. Verdier, *Biorheology*, 2010, **47**, 277–295.

26 J. Alcaraz, L. Buscemi, M. Grabulosa, X. Trepat, B. Fabry, R. Farré and D. Navajas, *Biophys. J.*, 2003, **84**, 2071–2079.

27 Y. Abidine, V. M. Laurent, R. Michel, A. Duperray, L. I. Palade and C. Verdier, *Europhys. Letters*, 2015, **109**, 38003.

28 Y. Abidine, A. Constantinescu, V. M. Laurent, V. S. Rajan, R. Michel, V. Laplaud, A. Duperray and C. Verdier, *Biophys. J.*, 2018, **114**, 1165–1175.

29 P. Sollich, F. Lequeux, P. Hébraud and M. E. Cates, *Phys. Rev. Lett.*, 1997, **78**, 2020–2023.

30 G. Massiera, K. M. V. Citters, P. L. Biancaniello and J. C. Crocker, *Biophys. J.*, 2007, **93**, 3703–3713.

31 J.-F. Palierne, *Rheol. Acta*, 1990, **29**, 204–214.

32 J.-F. Palierne, *Rheol. Acta*, 1991, **30**, 497.

33 D. Graebling, R. Müller and J.-F. Palierne, *Macromolecules*, 1993, **26**, 320–329.

34 A. Einstein, *Annals der Physik*, 1911, **34**, 591–592.

35 H. Nia, I. Bozchalooi, Y. Li, L. Han, H.-H. Hung, E. Frank, K. Youcef-Toumi, C. Ortiz and A. Grodzinsky, *Biophys. J.*, 2013, **104**, 1529–1537.

36 G. Helmlinger, P. A. Netti, H. C. Lichtenbeld, R. J. Melder and R. K. Jain, *Nat. Biotechnol.*, 1997, **15**, 778–783.

37 H. Byrne and L. Preziosi, *Math. Med. Biol.*, 2003, **20**, 341–366.

38 T. Stylianopoulos, J. D. Martin, V. P. Chauhan, S. R. Jain, B. Diop-Frimpong, N. Bardeesy, B. L. Smith, C. R. Ferrone, F. J. Hornicek, Y. Boucher, L. L. Munn and R. K. Jain, *Proc. Natl Acad. Sci. USA*, 2012, **109**, 15101–15108.

39 D. Ambrosi, L. Preziosi and G. Vitale, *Mech. Res. Commun.*, 2012, **42**, 87–91.

40 P. P. Provenzano, K. W. Eliceiri, J. M. Campbell, D. R. Inman, J. G. White and P. J. Keely, *BMC Medicine*, 2006, **4**, 38.

41 C. J. Whatcott, C. H. Diep, P. Jiang, A. Watanabe, J. LoBello, C. Sima, G. Hostetter, H. M. Shepard, D. D. Von Hoff and H. Han, *Clin. Cancer Res.*, 2015, **21**, 3561–3568.

42 M. Brooks, Q. Mo, R. Krasnow, P. L. Ho, Y.-C. Lee, J. Xiao, A. Kurtova, S. Lerner, G. Godoy, W. Jian, P. Castro, F. Chen, D. Rowley, M. Ittmann and K. S. Chan, *Oncotarget*, 2016, **7**, 82609–82619.

43 P. Royer, P. Recho and C. Verdier, *Mech. Res. Commun.*, 2019, **96**, 19–23.

44 E. M. Bindels, M. Vermey, R. van den Beemd, W. N. Dinjens and T. H. V. D. Kwast, *Cancer Res.*, 2000, **60**, 177–183.

45 L. Deng, X. Trepat, J. P. Butler, E. Millet, K. G. Morgan, D. A. Weitz and J. J. Fredberg, *Nat. Mater.*, 2006, **5**, 636–640.

46 P. Bursac, B. Fabry, X. Trepat, G. Lenormand, J. P. Butler, N. Wang, J. J. Fredberg and S. S. An, *Biochem. Biophys. Res. Commun.*, 2007, **355**, 324–330.

47 D. Stamenovic, N. Rosenblatt, M. Montoya-Zavala, B. D. Matthews, S. Hu, B. Suki, N. Wang and D. E. Ingber, *Biophys. J.*, 2007, **93**, L39–L41.

48 P. Cai, Y. Mizutani, M. Tsuchiya, J. M. Maloney, B. Fabry, K. J. V. Vliet and T. Okajima, *Biophys. J.*, 2013, **105**, 1093–1102.

49 G. Quarto, L. Spinelli, A. Pifferi, A. Torricelli, R. Cubeddu, F. Abbate, N. Balestreri, S. Menna, E. Cassano and P. Taroni, *Biomed. Opt. Express*, 2014, **5**, 3684–3698.